

## A Comprehensive Review for Integrating Petrophysical Properties, Rock Typing, and Geological Modeling for Enhanced Reservoir Characterization

Salam K Hasoon  , Ghanim M. Farman  \*

Department of Petroleum Engineering, College of Engineering, University of Baghdad, Baghdad, Iraq

### ABSTRACT

**R**eservoir characterization is an important component of hydrocarbon exploration and production, which requires the integration of different disciplines for accurate subsurface modeling. This comprehensive research paper delves into the complex interplay of rock materials, rock formation techniques, and geological modeling techniques for improving reservoir quality. The research plays an important role dominated by petrophysical factors such as porosity, shale volume, water content, and permeability—as important indicators of reservoir properties, fluid behavior, and hydrocarbon potential. It examines various rock cataloging techniques, focusing on rock aggregation techniques and self-organizing maps (SOMs) to identify specific and anomalous rock faces. Furthermore, the paper explores the adoption of advanced methods, including hydraulic flow units (HFU), providing a fine-grained understanding of reservoir heterogeneity and contributing to the prediction of flow dynamics. The final section includes structural geological models, petrophysical data collected, rock type classification, and spatial data to better represent the reservoir bottom structure. It provides a valuable resource for researchers, geologists, and engineers seeking to characterize reservoirs and make optimal decisions on hydrocarbon exploration and production. It is an important component of hydrocarbon exploration and production, which requires the integration of different disciplines for accurate subsurface modeling.

**Keywords:** Petrophysical characteristics, rock characteristics, conglomerate, soil models, and reservoir characteristics.

### 1. INTRODUCTION

The quest for improved reservoir characterization and subsequent efficient hydrocarbon recovery has driven the exploration of innovative techniques that bridge the gap between subsurface geological complexity and reservoir simulation accuracy. This comprehensive

---

\*Corresponding author

Peer review under the responsibility of University of Baghdad.

<https://doi.org/10.31026/j.eng.2024.10.05>



This is an open access article under the CC BY 4 license (<http://creativecommons.org/licenses/by/4.0/>).

Article received: 23/10/2023

Article revised: 08/01/2024

Article accepted: 03/03/2024

Article published: 01/10/2024



review delves into the synergy between petrophysical properties, rock typing methodologies, and geological modeling, showcasing their integral roles in achieving enhanced reservoir characterization and optimizing resource extraction (Aquino-López et al., 2015). Petrophysical properties, the fundamental attributes of reservoir rocks, form the cornerstone of subsurface analysis. Porosity, the fraction of void spaces within the rock matrix, profoundly influences fluid storage and movement. The volume of shale, a critical parameter in unconventional reservoirs, directly impacts hydrocarbon storage capacity and permeability (Ahmed and Farman, 2023a; Mahdi and Farman, 2023a). Water abundance and permeability, which are the natural conductive capacities of rocks are greatly affected because these factors are often geographically heterogeneous, which is important if absolute quantities are calculated and included in geological models to obtain estimates of dam performance Based on facts (Skalinski and Kenter, 2015). A basic method of classifying "rock types" classifies reservoir rocks into a number of groups according to their petrophysical properties. Clustering algorithms such as k-means clustering, hierarchal clustering, and self-organizing maps (SOM) using multidimensional petrophysical information provide effective tools for organizing related rocks into clusters. Rock properties enable complex reservoir models to be easily modeled by revealing hidden patterns and relationships, helping to develop better development strategies (Ahmed and Farman, 2023b; Mahdi and Farman, 2023c). In addition, a rock-type approach through core analysis, which integrates parameters such as Lucia Rock Fabric Number, Windland Classification, Hydraulic Flow Units (HFU), provides important insights into lake diversity and connectivity. This insight important for dynamic reservoir modeling (Qiu and Yi, 2023). The interface between reservoir engineering and subsurface geology is achieved through geologic models and enables accurate reservoir mapping. Building a subsurface stereographic from petrophysical characteristics and observations of rock properties is a process of developing a geologic model. This allows the structure of the reservoir to be observed, drainage identified, and flow pathways evaluated. The integration of petrophysical data with geological models will improve reservoir properties, leading to a better understanding of stratigraphic complexity, anisotropy and anisotropy (Qiu and Yi, 2023; Al Jawad et al., 2019). This review aims to demonstrate the importance of petrophysical properties as a basis for subsurface exploration, the effectiveness of rock-type techniques in weakening complex reservoirs, and their critical role which geological models play in bridging the gap between complex geology and reservoir engineering.

## 2. EVALUATION of FORMATION

Petrophysical characteristic analysis examines well logs in the context of a geologic concept. It uses a variety of data types for calibration, including core analysis, sedimentology, well-testing, and pressure data. Because these records provide precise measurements for constructing water vapor-rock relationships, computer programs can analyze and evaluate this data; Porosity, permeability and water saturation are not directly measured using well logs (Almazroui et al., 2020; Qiu and Yi, 2023).

### 2.1 Well Logging Techniques

The technique of continuously documenting different chemical, physical, electrical, or other aspects of the rock with depth is known as well logging. The petrophysical log created by a drill may be used to determine the mineralogy of potential reservoir rocks and the types of



fluids they contain, as well as to evaluate the deposition environment, petrophysical characteristics, and reservoir fluid distribution (**Qiu and Yi, 2023**). The following are some of the qualities that may be monitored by logging equipment:

- The rock's resistance at different distances from the borehole .
- The possibility for spontaneous rock/borehole fluid interface .
- The area absorbed by neutrons .
- The rock's acoustic distance between waves .
- The size of the rock-drilled borehole .
- The rock's density of electrons .
- Many other rock and well bore environmental aspects are connected to or derived from them.

## 2.2 Lithology and Mineralogy

In evaluating the formation, one of the most significant steps is to determine the lithology of the rock. Because it is impossible to detect porosity when the matrix is intact, the word "lithology" is employed to characterize the physical qualities of the material. Unknown location with unknown minerals or other unknown qualities. Numerous graphical approaches are regarded to be valuable tools. These methods give a way to comprehend the rock categorization in each formation, and they may be compared across different log readings to determine the porosity. Several different cross plots may be created in both two and three dimensions. (Density - Neutron and Neutron - sonic) Plotting is one of the oldest and most widely used ways of identifying lithology. This approach indicates the porosity matrix for the three primary forms of lithology: sandstone, limestone, and dolomite. Plotting may be visualized as lines marked with dots (**Burke et al., 1969**). **Fig. 1** shows the stratigraphic column in the Jurassic.

This illustrates a tick on the porosity scale. The position of the plotted points is used to depict the lithology (and mineralogy), and the positioning of the point varies from nonporous to porous rocks. At the same time, the shales appear at the boundary (**Bateman, 2020**).

The researcher in (**Díaz et al., 2016**) Used natural and pulsed neutron gamma-ray spectroscopy from open-hole observations, petrology and mineralogy in conventional and unconventional reservoirs. Gamma-ray spectroscopy in the casing holes is diluted by both concrete and casing, which increases measurement uncertainty and poses difficulties for coated aperture spectroscopy. By using correction procedures on data from pulsed neutrons and natural gamma rays, the elemental composition can be found. An interpretation system receives this data and uses it to determine the lithology and mineralogy of the formation. Coated hole findings are categorised lithologically and mineralogically in accordance with open-pit studies carried out in the basin's siliceous and carbonate layers. The data from jacketed holes can provide a table of contents for the formation. The use of casing and pulsed neutron generators helps to lower risks to health, safety, and the environment (HS&E) and encourages the collection of data in an eco-friendly manner. With the use of this innovative technique, operators may now get data that was previously limited to open pits, allowing them to better characterise the reservoir and increase output (**Díaz et al., 2016**).

Other researchers examined Lower Silurian transgression rock deposition in limited maritime environments. They are laterally discontinuous and regulated by palaeontological reliefs from glacial tectonic and Ordovician processes at the Gondwana scale. The fragments' analysis revealed minerals categorised into five groups: carbonate, mica, iron oxide, siderite,

clay, pyrite, chlorite, feldspar, and residual secondary minerals. The complicated distribution of TOC values and fragility in Lower Silurian “hot shales” may be due to their heterogeneity and vertical and lateral facies. Geochemical and mineralogical analyses of cutting samples will model source rock heterogeneity, forecast TOC levels and fragility, and assess shale gas potential (Burns, 2013).

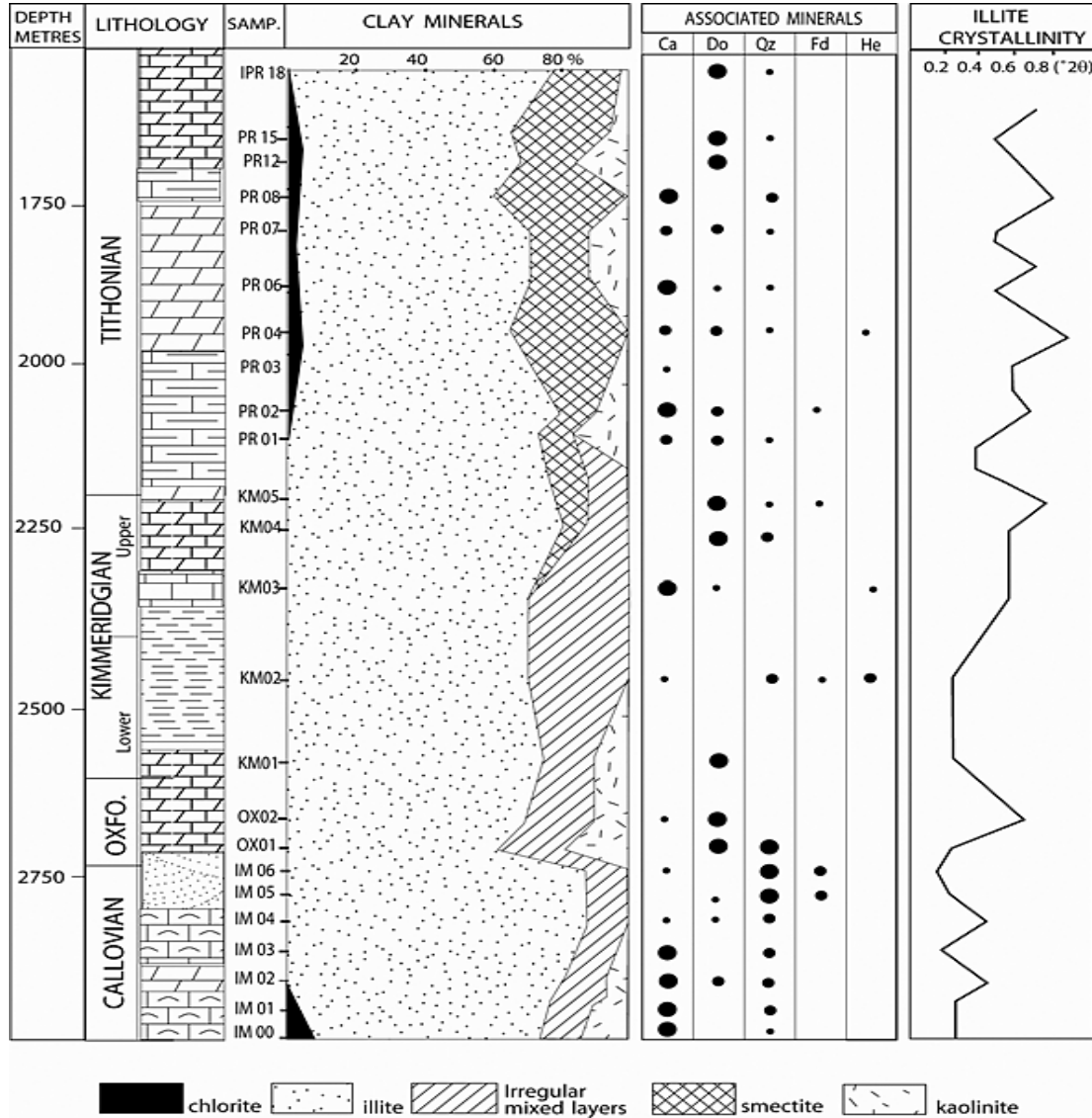


Figure 1. Lithology and clay mineralogy of the upper Jurassic Essaouira section (Burke et al., 1969).

### 2.3 Calculating the Amount of Clay Present

The presence of shale in the formation significantly impacts the rock's petrophysical properties, including a reduction in (both the total and effective porosity and permeability)(Kamel and Mohamed, 2006). In addition, the existence of shale introduces an element of uncertainty into the process of formation appraisal and the precise calculation of oil and gas reserves (Abudeif et al., 2016). Shale distribution affects the assessment of all primary reservoir properties, such as the effective porosity, water saturation, and



permeability (Aquino-López et al., 2015). Laminated clay, structural clay, and disseminated clay are the three categories that may be used to describe the distribution of clay within porous reservoir formations or any combination of these three categories:

- Clay particles are structurally crucial because they are scattered throughout the rock matrix, which they help to form.
- Clay dispersed throughout the clastic matrix can be found in open areas between the grains.
- Clay is layered very thinly between the sand units, creating a laminated structure.

The influence of shale mineral distribution on porosity is illustrated in **Fig. 2**.

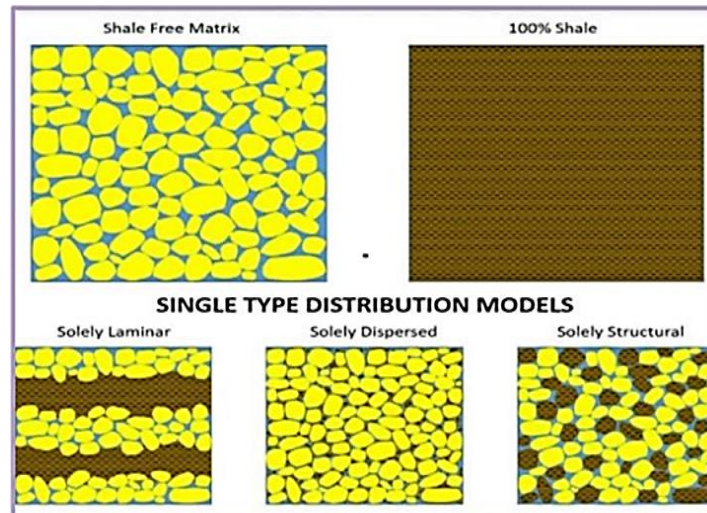


**Figure 2.** Different types of shale distribution affect the effective porosity of sandstone reservoirs (Ferguson et al., 2018).

The following is a list of the classic methods that are used in the petroleum business to determine the amount of clay:

### 2.3.1 Gamma Ray

Methods of Gamma rays are produced in response to the inherent radioactivity of the formation. Clay volume may be computed using the Gamma Ray using one of two methods: one technique assumes a linear response, while the other method assumes a curved response (Ngo et al., 2015). The GR is typically applied in situations when the volume of shale has to be defined ( $V_{sh}$ ) if the SP record is warped or if oil-based mud is utilized (Cannon, 2015). Larionov adjustment is referred to by the following equations, which apply to both consolidated and unconsolidated reservoirs (Mamaseni et al., 2018) :

$$V_{cl} = 0.330 * (2^{(2*IGR)} - 1) \quad \text{Consolidated} \quad (1)$$

$$V_{cl} = 0.083 * (2^{(3.7*IGR)} - 1) \quad \text{Unconsolidated} \quad (2)$$

where :

$V_{cl}$  is the clay volume.

IGR is the Gamma Ray Index.



### 2.3.2 Resistivity Method

The resistivity log is utilized to perform the calculation that determines the resistance of an electrical current as it moves through a formation. The two methods used to determine resistivity are sending a current into the formation directly or producing a current and measuring its resistance in ohms per meter. A current determines how great a reaction is produced at the detector **(Ahmed and Farman, 2023a)**. The effectiveness of the resistivity device when used as a clay identifier is determined by the difference between the resistivity response in shale and that of a clean pay zone. The fundamental equation is as follows **(Hussein and Ahmed, 2012)**:

$$Vcl = \left( \frac{R_{CL}}{R_t} * \frac{R_{LIM} - R_t}{R_{LIM} - R_{CL}} \right)^{\frac{1}{1.5}} \quad (3)$$

where:

$R_{cl}$  is the resistivity of clay (Adjacent Shale Bed).

$R_t$  is the resistivity of shaly sand.

$R_{LIM}$  is the resistivity of a clean hydrocarbon zone.

$Vcl$  is the volume of clay.

The resistivity approach is not guaranteed to produce reliable results for  $Vcl$  calculations; users should use caution when applying this method.

### 2.3.3 Neutron Method

Sending neutrons into formation to measure the formation's hydrogen content is what the neutron log does. This allows the hydrogen content to be measured. Below is a representation of the neutron equation that may be used to calculate the volume of clay **(Hussein and Ahmed, 2012; Ali et al., 2021)**:

$$Vcl = \frac{\phi(Nlog)}{\phi(Nclay)} * \frac{\phi(Nlog) - \phi(Nmin)}{\phi(Nclay) - \phi(Nmin)} \quad (4)$$

Where:

$Vcl$  is the volume of clay.

$\phi(Nlog)$  is the porosity measured from the neutron log at any depth.

$\phi(Nclay)$  is the porosity measured from the neutron log Infront of clay layers.

$\phi(Nmin)$  is the minimum porosity of the neutron log.

### 2.3.4 Sonic Method

The formation's laminar clay volume may be determined using the sonic log technique **(Hussein and Ahmed, 2012; Abdul-Majeed et al., 2020; Bateman, 2020)**. The acoustic equation that may be used to estimate the volume of clay can be found below **(Bassiouni, 1994)**:

$$Vcl = \frac{\phi S(Shaly Sand)}{\phi S(shale zone)} \quad (5)$$

where:

$Vcl$  is the volume of clay.



$\phi_s$  (Shaly Sand) is the porosity in the sonic spectrum at the shaly sand interval.

$\phi_s$  (Shale zone) is the porosity measurements taken at the shale interval.

### 2.3.5 Neutron-Density Method

This technique uses the neutron-land density response in shale to determine the amount of clay. The parameters of the clean matrix, precisely the neutron and density values of the sand, must either be known or assumed. The primary distinction When there is more clay present, the amount of space between neutrons and the density of the clay rises. The equation for estimating clay volume based on neutron density is shown in the equation **(Adeoti et al., 2009)**:

$$V_{cl} = \frac{\phi_N(\text{Shaly Sand}) - \phi_D(\text{Shaly Sand})}{\phi_N(\text{shale zone}) - \phi_D(\text{shale zone})} \quad (6)$$

Where:

$V_{cl}$  is the volume of clay,

$\phi_D$  (Shaly Sand) is the density and porosity in the zone of shale-like sand.

$\phi_N$  (Shaly Sand) is the porosity of neutrons in the zone of shaly sand.

$\phi_N$  (Shale zone) is the porosity measured using neutrons at the shale zone.

$\phi_D$  (Shale zone) is the density of the porosity is at the shale zone.

### 2.3.6 Sonic-Density Method

The presence of radioactive materials or fluid content did not noticeably impact the Sonic-Density technique. The equation for determining the volume of clay based on its acoustic density may be found below **(Adeoti et al., 2009)**:

$$V_{cl} = \frac{\phi_S(\text{Shaly Sand}) - \phi_D(\text{Shaly Sand})}{\phi_S(\text{shale zone}) - \phi_D(\text{shale zone})} \quad (7)$$

Where:

$V_{cl}$  is the volume of clay.

$\phi_s$  (Shaly Sand) is the porosity measured by neutrons at the shaly sand gap.

$\phi_D$  (Shaly Sand) is the density and porosity at the shale-and-sand interval.

$\phi_s$  (Shale zone) is the porosity measured using neutrons at the shale interval.

### 2.3.7 Neutron-Sonic Method

Because clay significantly impacts, the neutron-sonic equation that may be used to calculate clay volume is below **(Adeoti et al., 2009)**:

$$V_{cl} = \frac{\phi_N(\text{Shaly Sand}) - \phi_S(\text{Shaly Sand})}{\phi_N(\text{shale zone}) - \phi_S(\text{shale zone})} \quad (8)$$

Where:

$V_{cl}$  is the volume of clay.

$\phi_N$  (Shaly Sand) is the Porosity measured by neutrons at the shaly sand gap.

$\phi_s$  (Shaly Sand) is the porosity in the sonic spectrum at the shaly sand interval.

$\phi_N$  (Shale zone) is the porosity measured using neutrons at the shale interval.

$\phi_s$  (Shale zone) is the porosity measurements taken at the shale interval.

A crucial component of Petrophysics was addressed in the context of oil reservoir characterization. The main goal of this work is to create a technique for determining "useful porosity" in sandstone formations that contain a large amount of shale. The term "beneficial porosity" describes the porous portion that captures the presence of non-reservoir minerals, such as shale, and can effectively store hydrocarbons. Hosin's study addresses the problem of accurately assessing reservoirs due to the presence of shaly sandstone formations. Because traditional porosity estimates ignore reservoir minerals such as clay minerals in shale, which can limit suitable storage space for hydrocarbons, potential reservoirs are often overestimated. Another method of estimating useful porosity means that it considers the influence of mineral composition, shale content (**Hossin, 1965**). The theoretical and guiding principles of the Ensemble Kalman Filter were examined and discussed how empirical information can be used to develop new models of reservoirs. Case studies or numerical experiments can be provided to demonstrate the effectiveness and utility of the method in permeability and porosity calculations. This can include discussions on how to handle large amounts of data, deal with nonlinearity, and deal with uncertainties in reservoir parameters. The findings and results of the study could have a significant impact on how the oil and gas industry characterizes and manages its reservoirs. If proven successful, the ensemble Kalman filter could be a useful tool to enhance reservoir property estimation, which could ultimately lead to more accurate predictions of hydrocarbon reservoir behavior, and trajectories maintain the ponds (**Lorentzen et al., 2005**).

## 2.4 Porosity

If the lithology of the matrix is uncertain or if two or more minerals of unknown properties are present it may be difficult to obtain accurate matrix porosity readings. One and two log methods can be used to estimate porosity (**Hamada, 1996**). **Fig. 3** shows the types of porosity according to their percentage in the rock, and the percentage of porosity increased from left to right.

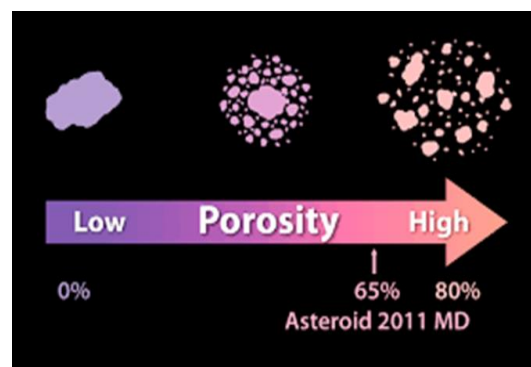


**Figure 3.** Solid as a rock porosity of asteroids (**Hamada, 1996**).

Using the Single log approach, porosity may be determined using density, sonic, and neutron measurements. Using the Double log method, effective porosity can be calculated by combining the Neutron Density and Neutron-Sonic log. The equation for the neutron density (**Mohamad and Hamada, 2017**) :

$$\phi_e = \frac{\phi_N + \phi_D}{2} \quad (9)$$





where:

$\phi_e$  is the Neutron-density logs' contribution to an effective porosity.

$\phi_N$  is the porosity as measured by the Neutron log.

$\phi_D$  is the porosity as a Function of the Density log.

The neutron-sonic equation may be used to determine the porosity of a material (**Mohamad and Hamada, 2017**):

$$\phi_T = \frac{\phi_N + \phi_S}{2} \quad (10)$$

where:

$\phi_T$  is the porosity that is achieved by the use of neutron-sonic logs.

$\phi_N$  is the porosity measured using the neutron log.

$\phi_S$  is the porosity measured with a Sonic log.

Akbar (**Akbar, 2019**) studied 67 sandstone and 120 carbonate core samples from Europe, Australia, Asia, and the US. Measured data for porosity  $\phi$ , permeability  $k$ , clay content  $V_{cl}$ , compressional velocity  $V_p$ , and quality factor  $Q_p$  under saturated and pressurised conditions are provided. After rearranging the Kozeny equation, pore geometry-structure (PGS) is presented for rock typing based on pore structural similarities. Rock typing can reveal the main parameters that affect acoustic velocity and quality factors. A novel solution to forecast porosity and permeability is also developed from basic rock physics equations for sonic velocity and critical porosity. The empirical formulae estimate compressional velocity and quality factors from petrophysical data. This work also develops empirical equations for porosity and permeability utilising compressional wave velocity, critical porosity, and PGS rock type. A trend analysis was used to simulate resistivity in hydrocarbon-bearing rocks using resistivity index-water saturation data and formation resistivity factor-porosity data. He eliminated  $R_0$  to blend the trends. This yields a useful empirical model for brine resistivity, porosity, water saturation, and rock bulk resistivity. Archie didn't mention any physics that may have supported his idea (**Kennedy, 2007**). They inspected Archie's Nacatoch sandstone data set to construct an alternate formula with a constant exponent of two and an adjustable percolation threshold. A similar but not identical formula was constructed using three fundamental principles (or self-evident axioms) and a percolation threshold-like parameter (**Kennedy and Herrick, 2012**). Further study has revealed that redefining porosity as "connected porosity participating in conduction" reconciles the seemingly conflicting formulae from 2007 and 2012 and brings the Archie model into accord with Kennedy and Herrick's models. The conclusion is equivalent to the Archie model with  $m = 2$  porosity exponent. This change makes Kennedy and Herrick's 2007 and 2012 formulations similar to the Archie equation. This is the first derivation of the Archie model from unambiguous first principles, applying Kennedy and Herrick's formula arguments to it and giving it a solid physical foundation (**Kennedy, 2016**).

## 2.5 Formation Water Resistivity

When attempting to determine hydrocarbons in situ from wireline logs, one of the essential metrics required is the connate water resistivity, also known as  $R_w$ , in the formation of interest. Connate water is not tainted by any other types of contaminants (**Mabrouk et al., 2013**). Muck from drilling has completely soaked the porous rock structure. Because it is



necessary for deriving saturations (of either water or hydrocarbon) from basic resistivity logs, the formation of water resistivity is an essential interpretation parameter. On the other hand, numerous methods for determining the resistivity of the reservoir water have been developed. These methods include chemical analysis of the produced water sample, direct measurement in a resistivity cell, water data logs, the spontaneous potential (SP) curve, resistivity porosity logs, and various empirical methods (**Mabrouk et al., 2013**).

### 2.5.1 Formation of Water Resistivity by Spontaneous Log

This approach is one of the most significant and extensively used ways for determining  $R_w$  from the SP log. This method depends on the connection between  $R_w$  and SSP, as stated in Eq. (11). The  $R_w$  values derived from such sources as Conventional SP analysis produce consistently poor results when compared with  $R_w$  from natural water samples or  $R_{wa}$  analysis derived from sonic and resistivity logs (**Policky and Iverson, 1988**).  $R_w$  was formerly obtained by the traditional SSP equation, which is as follows:

$$SSP = -(60 + 0.133 Tf) * \log\left[\frac{R_{mf}}{R_w}\right] \quad (11)$$

where:

SSP is the log static and spontaneous recording at precise intervals (MV).

$R_w$  is the water's resistivity during formation (ohm-m).

$R_{mf}$  is the resistance of the filtrate from mud (ohm-m).

The methodology and techniques employed to extract water resistivity information from SP logs were discussed in (**Policky and Iverson, 1988**). They may explain how SP logs are sensitive to changes in formation water properties and how these measurements can be calibrated and interpreted to estimate water resistivity values. The study may include case studies or examples from the Minnelusa Formation in the Powder River Basin to illustrate the practical application of the proposed method. These examples may showcase the challenges and successes of estimating water resistivity in real-world reservoir scenarios. This novel method gives more accurate hydrocarbon potential estimates for prospective intervals in this deposit (**Policky and Iverson, 1988**).

A novel sensor technology was designed to measure formation water resistivity in subsurface reservoirs precisely. This research represented a significant advancement in well-logging and petrophysics. The primary focus of this study was developing and calibrating a specialized sensor that accurately measures the resistivity of water formation in oil and gas reservoirs. Formation water resistivity is a crucial parameter in reservoir characterization used to assess reservoir properties, fluid type, and the potential for hydrocarbon production. The sensor's induction-based operation avoids electrodes and measurement fouling from particle coating or buildup. Resistivity measuring precision and resolution allow direct comparison of guard and sample flowlines during focused sampling, even when filtrate and formation water contrast is minimal. As proven in another PDO trial, the data may be utilised directly to measure  $R_w$  in exploratory scenarios, compared to other  $R_w$  measurement sources, or used to increase the accuracy of alternatives to the Archie equation, such as dielectric dispersion (**Chen et al., 2020**).



## 2.6 Archie Parameters

The use of volumetric methodologies necessitates collecting petrophysical data, such as porosity and water saturation, to determine the amount of hydrocarbons already present (**Bose et al., 2019**). Archie conducted an independent study in 1941 that already determined the amount of water in hardened sand dunes. This formula relied on several construction characteristics such as porosity and construction resistance (**Kennedy and Garcia, 2019**). Methods for finding Archie parameters have been tested and validated for use in sandstone reservoirs. On the other hand, the texture and pore size of rice sands can vary greatly from place to place. Errors in the calculated concentrations will be due to uncertainties in these parameters, which are not allowed (**Mohamad and Hamada, 2017**). To obtain an overview of the ARCHI parameters, Wael Abdullah et al. (2023) provided a framework that combines well-log data with laboratory measurements. Their approach provided a more accurate understanding of the electrical properties of a reservoir by overcoming the shortcomings of traditional methods that rely on discrete measurements. A case study was presented to illustrate how this approach calculate the Archie parameters correctly. The process data provided important information about reservoir characteristics, which contributes to quality product development and reservoir quality (**Abdallah et al., 2023**). The finite element method was used to model the behavior of groundwater and rock outcrops. The Archie parameters  $m$  and  $n$  were calculated using the solution of the system. In addition, a machine learning method was presented in the study to obtain ARCHI parameter information from dielectric measurement analysis. The findings of the study showed that both methods are independent and provide reliable estimates of ARCHI parameters to so. This has important implications for how groundwater management and other subsurface applications are designed, and how intercept data are interpreted the results have been valid for carbonates, sandstones and lithologies. When the alternative  $m$  and  $n$  are used to interpret resistivity data for core plug water saturation, the average uncertainty is reduced from 13% to 4% (**Al-Ofi et al., 2022**).

### 2.6.1 Cementation Factor ( $m$ )

One of the most important archachars for determining the amount of water in a particular reservoir situation is the cementing factor, which also contributes significantly to the uncertainty of the process (**Shahi et al., 2018**). The cementation factor varies depending on the sample, the formation, or the interval. It has been observed that the density of crushed sandstone ranges from little less than one to more than three, which accounts for the figure form for fractured rock. The cementation exponent is largely determined by the structure and shape of the pores and grains, as opposed to the rock's tortuosity, specific surface area, and anisotropy (**Salem and Chilingarian, 1999**).

### 2.6.2 Pickett Plot

This is one of the most typical methods used to determine the cementation factor ( $m$ ) from well logs. The assumption that " $m$ " is unknown provides the foundation for this plot and allows us to employ an Archie connection (**Pickett, 1966**). **Fig. 5** shows the diagram between resistivity and  $(\rho_m - \rho_b)$  for extracting  $m$ ,  $n$ ,  $a$ ,  $R_w$  and  $S_w$ .

$$Rt = \frac{a \cdot R_w}{\phi^m \cdot S_w^n} \quad (12)$$



where:

$R_t$  is the Deep resistivity (ohm-m), formed through formation,

$a$ ,  $n$  and  $m$  are Archie parameters (dimensionless).

$R_w$  is the Water's resistivity, measured in (ohm-m).

$\phi$  is the porosity.

$S_w$  is the saturation (fraction) of the water.

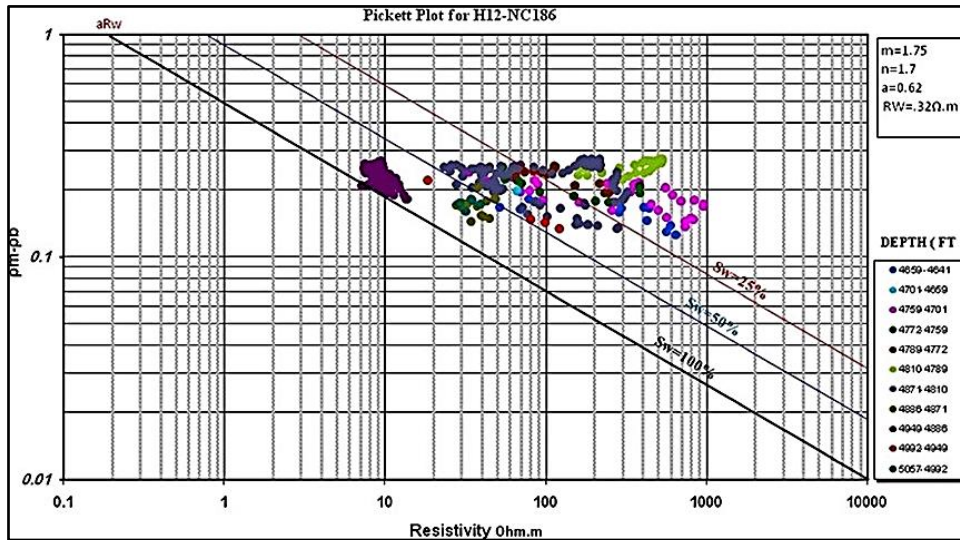


Figure 5. Pickett's plot (Pickett, 1966).

When logarithms are applied to both sides of the equation (12), the result is the following:

$$\text{Log } R_t = -(m)\text{log}( \phi ) + \text{log}(a \cdot R_w) - n\text{log}(S_w) \tag{13}$$

During a period that included water,  $S_w = 1$

$$\text{Log } R_t = -(m)\text{log}( \phi ) + \text{log}(a \cdot R_w) \tag{14}$$

The equation (14) represents a straight line in log-log coordinates and takes the form ( $Y = mx + b$ ). In this equation, the slope will be denoted by "m," and the intersection will be denoted by  $(a \cdot R_w)$ , where "a" will always equal unity. In a regular Cartesian coordinate system, the values along the axes increase linearly. However, in a log-log coordinate system, the values increase exponentially. Each tick mark on the axis corresponds to a power of the base of the logarithm. For example, in a base 10 logarithmic scale, the tick marks would be located at 1, 10, 100, 1000, and so on (Pickett, 1966). A tortuosity factor of 1 indicates that there is no tortuosity present in the path. It means that the path follows a direct and linear trajectory from its starting point to its endpoint, without any obstructions, bends, or irregularities (Pickett, 1966).

### 2.6.3 Saturation Exponent (n)

The saturation exponent (n) is a dimensionless empirical measure of electrical reservoir rock attributes that establishes the link between the water saturation of rock and the actual resistivity of fluid-filled rock to estimate reserve hydrocarbon saturations (Al-Hilali et al.,

**2015).** As a result of core analysis, it has been discovered that the assumption of ( $n=m$ ) in irreducible water levels. A new petrophysical approach was presented employing water saturation, absolute resistivity, and total reservoir porosity data; geological stratification is essential. Pickett diagrams and Sw-Phi diagrams were used to plot irreducible water saturation factors and consolidation exponents for each region. The link between true formation resistivity ( $R_t$ ) and reservoir porosity in irreducible water saturation intervals was mathematically derived to forecast the saturation exponent using a cross plot. Their research introduced a unique petrophysical approach combining water saturation, absolute resistivity, and reservoir total porosity data. Geological stratification is essential. The suggested model was tested using case studies from three substantial oil fields in southern Iraq to reflect distinct application situations for oil-bearing carbonate and shale sand formations. the petrophysical procedure proposed for this study was simplified and robustly determined the water saturation exponent ( $n$ ), and improved water saturation ( $S_w$ ) estimated values and may be used in carbonate or sand shale reservoirs **(Al-Hilali et al., 2015)**. The permissible range was re-examined for the saturation exponent 'n' in well-log interpretation. They analyzed various theories, models and equations related to the saturation exponent and evaluated its significance in determining the water saturation in a reservoir. The authors suggested that the range of 'n' values currently used in well-log interpretation may require reconsideration and offer a new method for calculating the optimal range for 'n' in different rock types. However, decades of core and open hole log analysis indicated n larger than one and usually two .Most studies agreed that wettability and saturation history (drainage or imbibition) impact saturation exponent. Several publications report n values from 1 to 20 for heavily oil-soaked rocks. Too frequently, assumptions are accepted .This research analysed the link between water saturation and rock resistivities to establish n's relevance and provide ways to improve an assumed value **(Adisoemarta et al., 2001)**.

#### 2.6.4 Tortuosity Factor ( $\tau$ )

The term "tortuosity" refers to the ratio of the actual length of the flow route to the length of the porous medium in a direction perpendicular to the direction of the flow as a whole **(Winsauer et al., 1952)**. the usual starting point for the tortuosity factor of a sandstone reservoir is 0.6; however, this number might shift when matching log data with other data sources such as core **(Mazzullo et al., 1996)**. **Fig. 6** shows the relationship between porosity and Tortuosity.

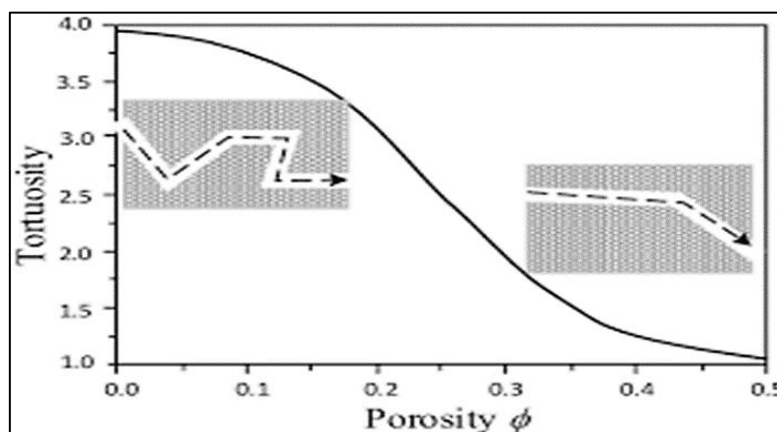


**Figure 6.** Effect and value of tortuosity factor **(Winsauer et al., 1952)**.





## 2.7 Water Saturation

The term "water saturation" refers to the percentage or pore volume fraction filled with a given fluid (water in this case). This attribute may be expressed using the mathematical connection shown below (Archie, 1950) :

$$S_w = \frac{\text{volume of fluid in pores}}{\text{volume of pores}} \quad (15)$$

Archie (1950) observed and addressed porosity-electrical resistance correlations in porous media. He developed equations to determine fluid saturations, quantifying well-log assessment. In 1950, G.E. Archie examined sedimentary settings, rock types, and petrophysical factors and recommended focusing on cap rocks and reservoir rock properties to create Petrophysics, a geologic discipline (Archie, 1950).

$$S_w^n = \frac{a \cdot R_w}{\phi_T^m \cdot R_t} \quad (16)$$

where:

$S_w$  is the water saturation.

$n$  is the saturation exponent.

$a$  is the tortuosity factor.

$R_w$  is the resistivity of formation water, (ohm-m).

$\phi_T$  is the porosity.

$m$  is the cementation factor.

$R_t$  is the true formation resistivity, (ohm-m).

Equation (15) is an appropriate equation to compute the water saturation in reservoir rocks. The findings were presented using the resistivity approach, which makes this equation a recommended equation for calculating the amount of oil in place (Adeoti et al., 2009). Simandoux (1963) used a dependable model to forecast water saturation during the creation shaly sand. The technique based on experimental data of uniform mixtures of sand and montmorillonites commonly found in complicated reservoir rocks. The Simandoux model is still among the most often used for calculating water saturation (Simandoux, 1963). Morris and Biggs (1967) explored the link between "porosity-water saturation" (also known as the Buckles number), which is a constant expressed as a percentage of bulk water volume (BVW). Using this constant, Separate transition layers from one another at approximation permeability and irreducible saturation. Water saturation ( $S_w$ ) vs porosity is displayed on a Buckles plot (Morris and Biggs, 1967). Timothy O. Pius et al (2020) examined the relationship between the produced water cut and the average water saturation around the perforation as measured by the Cased-Hole Saturation Tool (CHST). This project aimed to save money by reducing CHST logging runs for Reservoir Fluids Management. For Niger Delta wells with lengthy perforation intervals (> 30 feet), generated water cut correlates enormously with average water saturation. However, average water saturation strongly correlates with water cut and interval thickness for North Sea Basin wells with short perforation intervals (10–30 feet). Obviously, empirical correlations were unattainable for wells abandoned for more than four months. The discrepancy between water production and average water saturation may be due to petrophysical property variability and borehole reinvasion (Pius and Olamigoke, 2020).



## 2.8 Permeability

Permeability: the capacity of the rock to transfer fluid is one of the most essential features in reservoir characterisation. This property is considered a vital key for reservoir modelling and determining well-completion design and developed reservoir management techniques for improved oil extraction. Even in rocks with excellent porosity and irreducible water saturation, the flow would be pending without permeability, in addition to the presence of fluid viscosity and pressure gradient. Permeability is another phrase for the flowing ability of the formation. The tensor element known as "permeability" has an array of components that are mostly an anisotropy for the horizontal ( $K_h$ ) and vertical ( $K_v$ ) directions. The permeability might be expressed by Darcy's equation, which is as follows **(Schön, 2015)**.

$$q = \frac{0.001127kA(p_1 - p_2)}{\mu L} \quad (17)$$

where:

- q is the flow rate, bbl/day.
- k is the absolute permeability, md.
- p is the pressure, psia  $\mu$ = viscosity, cp.
- L is the distance, ft.
- A is the cross-sectional area, ft<sup>2</sup>.

Kun Su et al (2022) described the results of experiments in low-permeability carbonate reservoirs prior to salinization. These reservoirs were tested under stress to evaluate the short-term and long-term effects of acid treatment and proppant application on bladder permeability. The authors found that proppants held the bladder well when over time, while acid therapy proved ineffective. These findings may improve hydraulic fracturing techniques in pre-salt low-permeability carbonate reservoirs for better management and increased production **(Su et al., 2022)**.

### 2.8.1 Classical Method

Methods such as testing well logs and measuring core samples are commonly used in assessing formation permeability. Using the empirical relationship between permeability and porosity, this method can determine permeability from porosity directly. A porosity and permeability model were constructed from the core data. Well sections can be used to predict permeability in noncores **(Taslimi et al., 2008)**. The general form of the traditional permeability-porosity relationship is usually expressed as follows:

$$\log K = a \phi + b \quad (18)$$

- k is the permeability (MD).
- $\phi$  is the porosity (fraction) and a and b are the slope and intercept, respectively.

### 2.8.2 Hydraulic Flow Units

In petrophysical reservoir description, the Hydraulic Flow Unit (HFU) approach has been utilised as an integrating tool to categorise rock types and estimate flow parameters. The widespread challenge of predicting permeability in uncored yet logged wells served as the



impetus for the development of the HFU technique (Svirsky et al., 2004). If the (FZI) of the reservoir rock is known, then this approach will offer correct correlations between the porosity and permeability of the rock. FZI is often applied to uncored wells through correlations with log characteristics after being calculated from core data in cored wells. However, FZI may also be computed directly from core data (Ngo et al., 2015).

### 2.8.3 Reservoir Quality Index (RQI)

Amaefule was the one who first considered both the permeability and the porosity of the reservoir when developing the idea of the reservoir quality index, or RQI. In general, the quality of a reservoir is determined by two characteristics: storage capacity (porosity), permeability (flow capacity), and capacity (load bearing). When calculating hydraulic flow units in a reservoir, porosity and permeability are crucial elements. The porosity-permeability relationships determined from the actual measurements of rock samples taken from cored wells are used to make an approximation of the permeability of wells that have not been cored. The Reservoir Quality Index, often known as RQI, is a property that was defined by Amaefule et al. (1993) using the correlation (Wang et al., 2014):

$$RRQI = 0.314 * \sqrt{\frac{K}{\phi_e}} \quad (19)$$

where:

RQI is the Reservoir Quality Index.

K is the Permeability, (md).

$\phi_e$  is the effective porosity, (%).

$\sqrt{\frac{K}{\phi_e}}$  is what's referred to as the rock's hydraulic diameter.

RQI was calculated using the porosity-permeability values found in the core samples.

### 2.8.4 Flow Zone Indicator (FZI)

The Flow Zone Indicator is a one-of-a-kind and beneficial value that provides a link between petrophysical features at small-scale, such as core plugs, and large scale, such as the level of the well bore, to quantify the flow character of a reservoir (Yarmohammadi et al., 2013). Fig. 7 shows a drawing between FZI and Depth.

In addition, the modelling of flow zones based on surface area and Tortuosity is what's meant to be referred to when using the term FZI (Al-Dhafeeri and Nasr-El-Din, 2007). Another attribute of the rock that was determined by its textural characteristics and grain size was called the Flow Zone Indicator, or FZI. This property was characterized as:

$$FZI = \frac{RQI}{\phi_z} \quad (20)$$

where:

FZI is the Flow Zone Indicator.

RQI is the Reservoir Quality Index.

$\phi_z$  is the Normalized porosity.

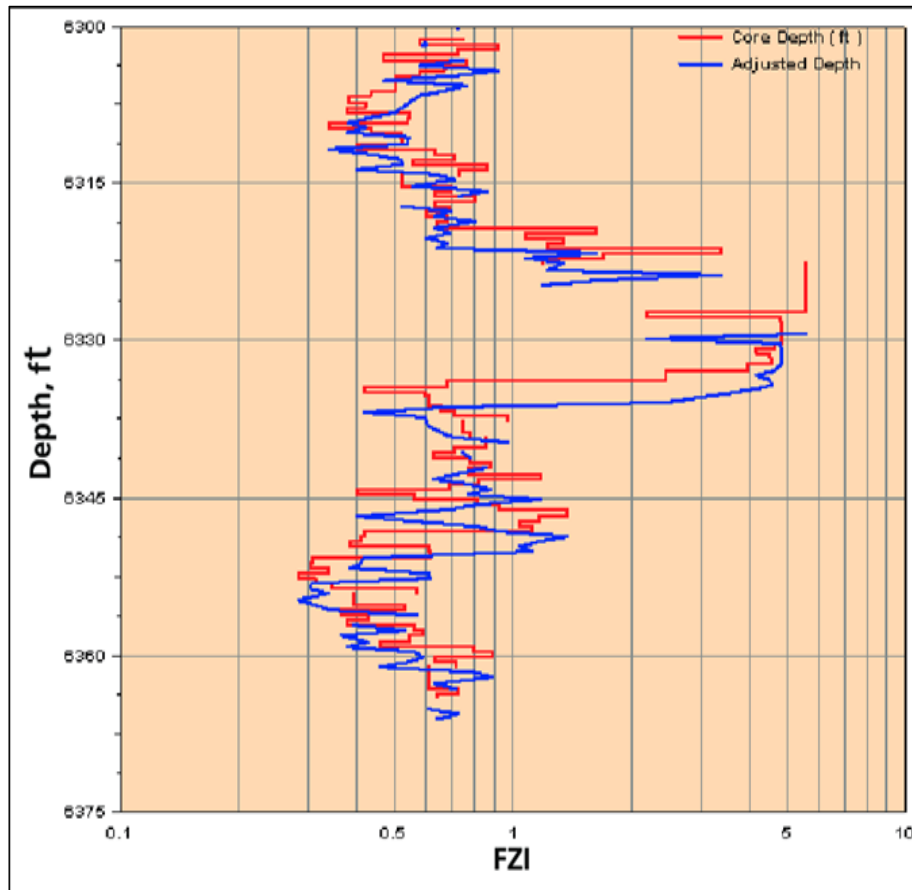


**Figure 7.** Flow zone indicator (FZI) correlated with adjusted core and drilling depth (Al-Dhafeeri and Nasr-El-Din, 2007).

The ratio of pore volume to grain volume is the definition of normalised porosity, and the formula for calculating it is as follows:

$$\phi_z = \left[ \frac{\phi_e}{(1-\phi_e)} \right] \quad (21)$$

where:

$\phi_e$  is the effective porosity, (%).

$\phi_z$  is the normalized porosity.

### 2.8.5 Winland Method

The concept of pore throat radius was utilized by Winland (1972) to categorize the various sorts of rocks. Once the size of the pore throat matches an accumulative mercury saturation curve of 35%, the Winland empirical relation demonstrates the most robust statistical correlation. R35 refers to the pore throat radius (Kolodzie Jr, 1980).

The following is an explanation of the Winland equation, which Kolodzie (1980) utilized and published:

$$\text{Log R35} = 0.732 + 0.588 * \text{log K air} - 0.864 * \text{log } \phi \quad (22)$$

$K_{air}$  is the permeability determined using air pressure (md).

$\phi$  is the amount of porosity (in per cent) the rock has.

R35 is the amount of mercury that has filled the pore throat, at a size of 35 per cent.

The rocks that make up a reservoir are divided into several different rock types or hydraulic flow units, and these classifications are based on the fact that rock samples from the same rock type have a comparable R35 and lie on an iso-pore throat curve **Fig. 8 (Ali et al., 2021)**.

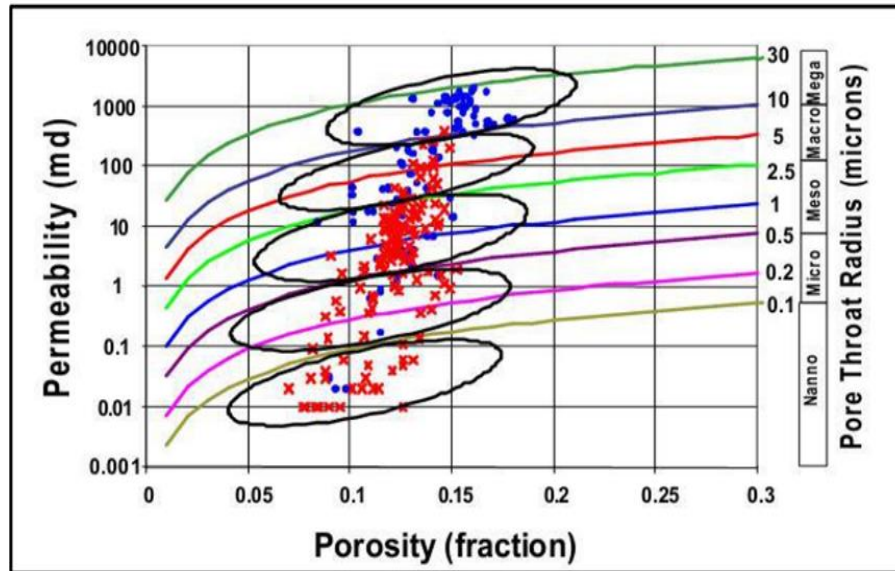


**Figure 8.** Five rock types were constructed using the Winland correlation (Porrás et al., 2001).

From the reservoir rock, it is possible to create the following five petrophysical groups:

- Mega pores: which have a pore throat radius that is higher than 10 microns.
- Macro pores have a hole throat radius ranging from 2.5 to 10 microns.
- Meso pores: having a pore throat radius between 0.5 and 2.5 microns.
- Micro pores: having a pore throat radius between 0.2 and 0.5 microns.
- Nanopores: having a pore throat radius that is lower than 0.2 microns.

### 2.8.6 Lucia Method

Rock permeability and saturation are both governed by the porous structure of the rock, and the Lucia classification characterizes the spatial distribution of pores of different sizes inside that rock. The pore space in carbonate rock textures may be related to the pore-size distribution of the rock if the pore space is characterized as either interparticle, separate-vug, or touching-vug, depending on the kind of pore (Lucia et al., 2003). **Fig. 9** shows the relationship between porosity and permeability.

Lucia's Petrophysical Rock Classification uses laboratory measurements of porosity and permeability. These measurements relate pore size distribution to the number of rock fabrics in a given sample (Bhatti et al., 2020). Rock fabric number is a formula (22) provided by Lucia (2007) (RFN) **Fig. 10**

$$\log(k) = (9.7982 - 12.0803 \log \text{RFN}) + (8.6711 - 8.2965 \log \text{RFN} \log \phi). \quad (23)$$



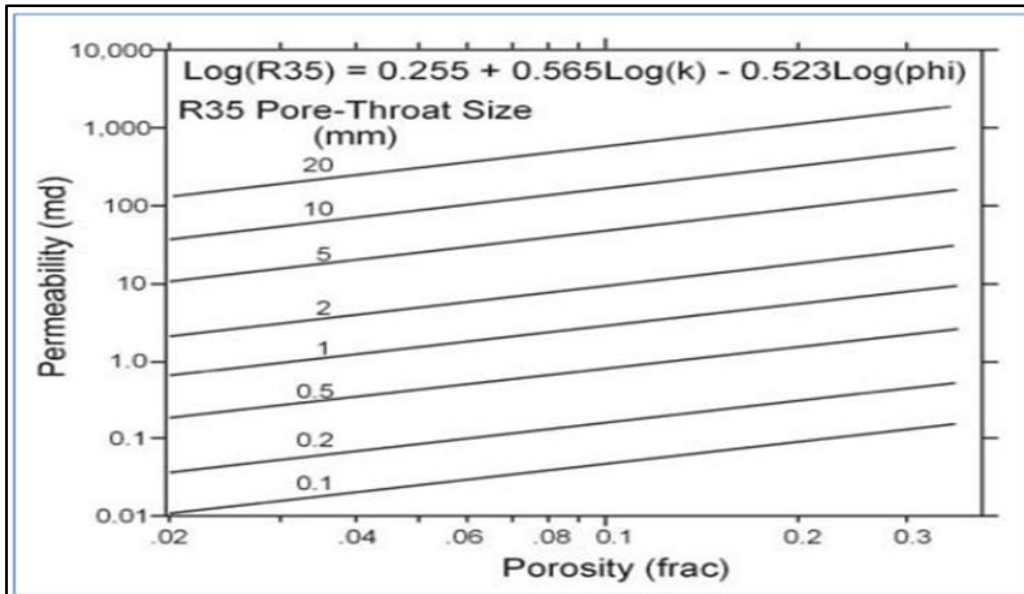


Figure 9. Pore throat radius classification(Pittman, 1992).

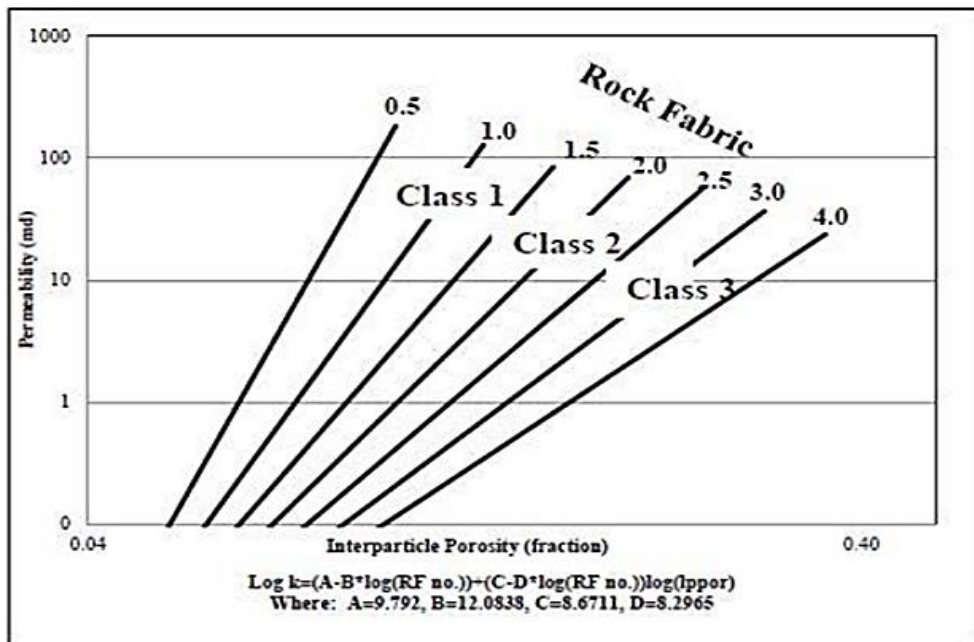


Figure 10. Rock fabric number classification(Riazi, 2018).

### 2.9 Cutoff Determination by Sensitivity Analysis

After using the cutoff values for input petrophysical characteristics like average porosity and average water saturation values to determine hydrocarbon volume in an area, the cutoff is the process of forecasting the net pay thickness (Singh and Joshi, 2020). The adequate flow thickness of the reservoir may be distinguished, which helps to identify the specific interval, remove zones with tight porosity or low porosity, and eliminate intervals with excessively high-water saturation. This information can then calculate net pay (Paul and Gaffney, 2003). On the other hand, if the cutoffs were entirely removed, the average values of porosity and water saturation would rise, and the net thicknesses would also rise. If rocks of



low grade are utilised in the construction of the computation of the average characteristics of the reservoir shows that the obtained values of average porosity and water saturation are lower than expected (Kolodzie Jr, 1980). A sensitivity analysis method was used in this study (Ali et al.,2021). This method is a tool used in economic modeling to analyze the effect of different terms of an independent variable on a particular dependent variable for the satisfaction of particular criteria (Wang et al., 2014). Fig. 11 Draws a graph between Vsh and Eqv, and the optimal Vsh cutoff is determined by the graph; Fig. 12 Draws a graph between the porosity cutoff and Eqv, and the optimal porosity cutoff is determined by the graph; Fig. 13 Draws a graph between the Sw cutoff and Eqv, and the optimal Sw cutoff is determined by the graph.

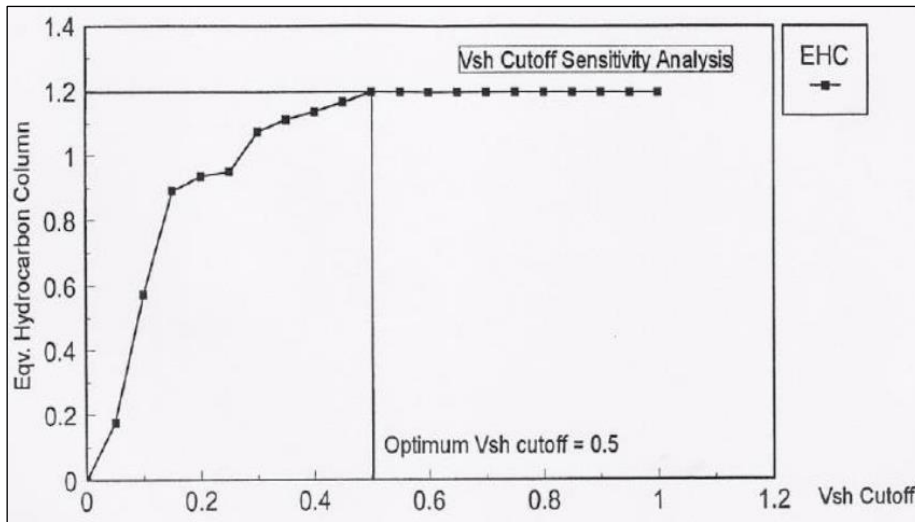


Figure 11. Shale volume cut-off sensitivity analysis (Kyi, 2019).

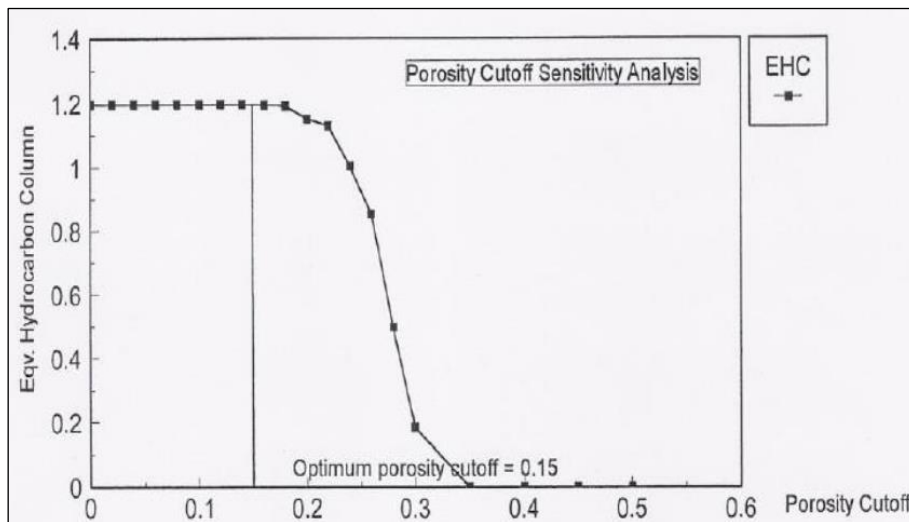


Figure 12. Porosity cut-off sensitivity analysis (Kyi, 2019).

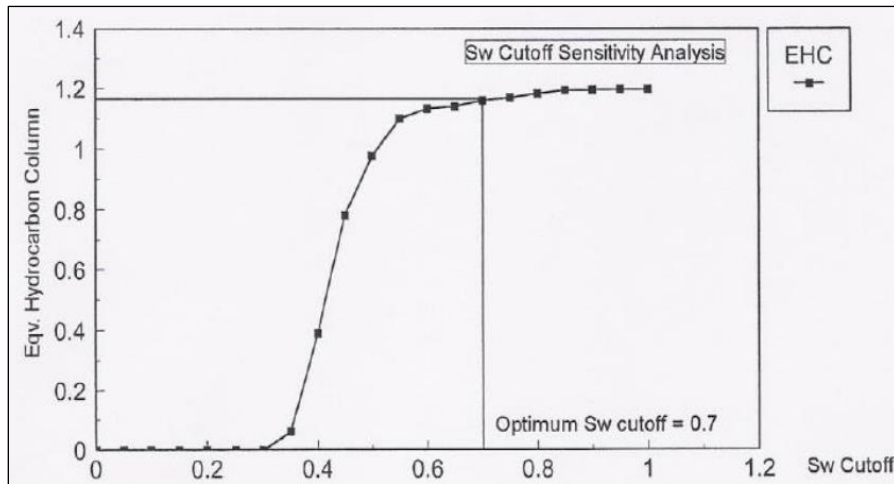


Figure 13. Water saturation cut off sensitivity analysis (Kyi, 2019).

## 2.10 Cluster Analysis

Cluster analysis is a multivariate approach that seeks to split the data based on a single variable into several groups with comparable subjects in the same group. This data division is accomplished via a clustering algorithm (Cornish, 2007). The approach known as "well log cluster analysis" classifies data points according to their electrofacies by comparing and contrasting the similarities and differences among them in the multivariate space of logs (Al Kattan et al., 2018). The k-means method is one of the most used and straightforward approaches to grouping data (Abed and Hamd-Allah, 2019; Abdulkareem et al., 2020). It is preferred over alternative techniques because of its effectiveness in clustering big data sets and the speed with which it converges to acceptable results in various applications (Mihai and Mocanu, 2015). This produces the desired results in the following steps:

- Defining the number of clusters that will be established using k-means is the first step in assigning the group size, or K. It was determined by the original predicted number (20) to involve the most significant quantity of different data.
- Distance Measurement (Similarity/Dissimilarity): In this stage of the k-means method, the goal is to minimise the sum of squares difference within the same cluster between the k-main centroids and the n objects of log data points. This is accomplished by using a similarity/dissimilarity matrix. Things located within the same cluster are more similar and closer to one another than objects located inside other clusters.
- Data grouping: Agglomerative (hierarchical) cluster analysis was used to organise the data in groups by merging the related clusters and performing computations until one cluster was obtained (Doveton, 1994).
- The definition of the randomness index is shown in the preceding (Hasan, 2021):

$$\text{Randomness index} = \frac{\text{Average Thickness}}{\text{Random Thickness}} \quad (24)$$

where:

$$\text{Average Thickness} = \frac{\text{Number of depth levels}}{\text{Number of cluster layers}} \quad (25)$$

### 2.11 Electrical Rock Type

Electrical flow units, often known as EFUs, are zones with electrical characteristics comparable to one another. They are distinguished by a current zone indicator, often known as a CZI (**Rezaee et al., 2008**):

$$CZI = \sqrt{\frac{\phi/F}{\varepsilon}} \quad (26)$$

where  $\phi$ ,  $F$ , and  $\varepsilon$  are porosity (fraction), formation factor, and the pore-to-matrix volume ratio, abbreviated as (PMR), respectively. Calculating the electrical radius indicator (ERI) involves the following steps:

$$ERI = \sqrt{\left(\frac{\phi}{F}\right)} \quad (27)$$

Then,

$$CZI = \frac{ERI}{\sqrt{\varepsilon}} \quad (28)$$

The CZI is a factor that may be used to differentiate between reservoirs that have almost identical  $m$  and values and in which the difference in  $F$  is a function of porosity. Each sample that falls within a certain CZI range has a set of units that have been suggested to have the same electrical flow parameters (**Rezaee et al., 2008**). A technique based on electrical flow units was used for a deep sandstone reservoir at the Shah Deniz gas production. The principal reservoirs are known as Balakhani VIII and sandy packages II and III of the Fasila group. Their findings demonstrated a correlation between high reservoir quality units and high CZI zones **Fig. 14** (**Yarmohammadi et al., 2013**).

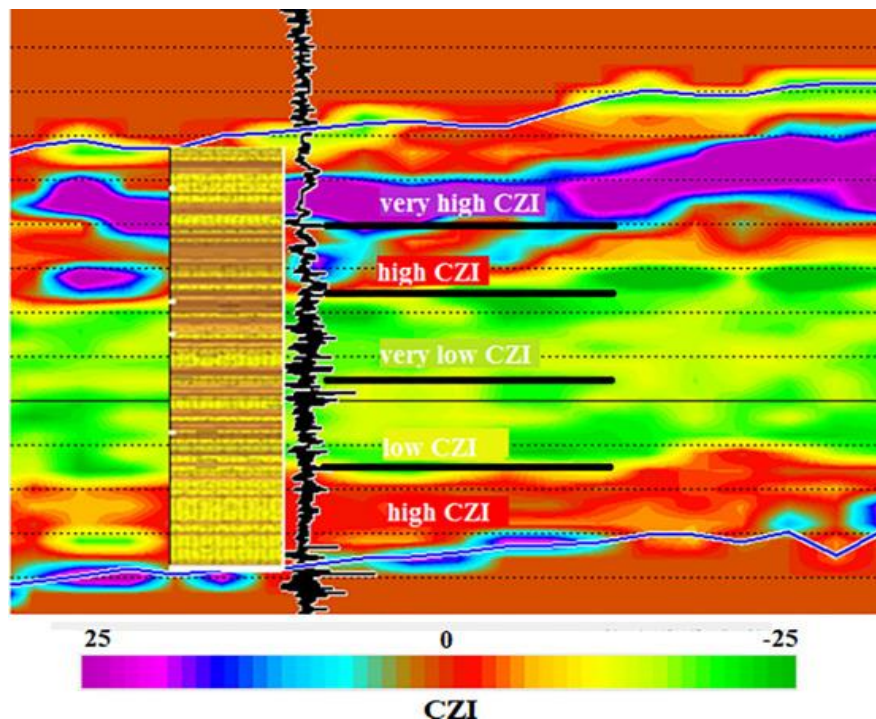


**Figure 14.** A 2D section of CZI distribution correlated with a lithological column in well SDX-04, Shah Deniz gas field; Good pay sandstones correspond to high CZI values (**Yarmohammadi et al., 2013**).

## 2.12 Geostatistical Analysis

Geostatistics is a modern, influential method for reservoir description and seismic inversion. It is also utilized for predicting soil conditions at sites that have not been visited and for mapping based on sample survey data. The methodology is predicated on models of the variations that occur in space. It is assumed that soil qualities are the results of random processes that are geographically linked, and it is possible to add the fixed effects of geographic trends or correlation with other environmental factors to this assumption (Almazroui et al., 2020). Geostatistics aims to make predictions about geochemical, geophysical, and other natural variables by seeing these variables as realizations of a stochastic process, either in a two-dimensional plane or a three-dimensional space (Nielsen, 2009). The first step in the prediction process is the estimate of spatial covariance or semivariograms, to which feasible variogram models are fitted. The second step in the prediction process is the kriged predictions, which are based on the previous step's results. The simulation of the variogram models is presented in Fig. 15. During the simulation process, numerous equal likelihood maps of the property distribution are constructed. This is accomplished by employing the same model of spatial correlation that is necessary for Kriging (Wang et al., 2014). Geostatistical models have been playing an increasingly important role in groundwater hydrology and in the modeling of petroleum reservoirs. It offers intriguing answers to the two significant issues. The putting together of dimensional geologically accurate representations of heterogeneity in three petrophysical characteristics and the measurement of uncertainty through the production of many alternative models are included in this study (or realizations) (Hosseini et al., 2019).

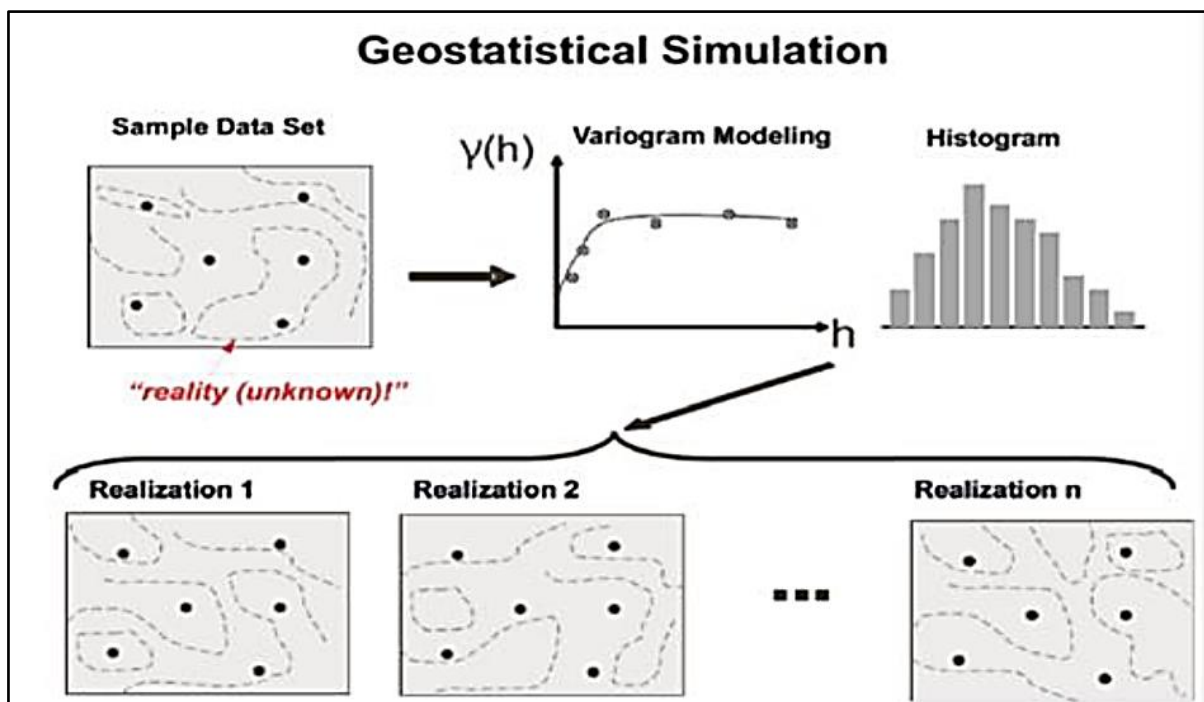


Figure 15. Geostatistical simulation workflow (Salman et al., 2023).

A case study from the Zubair Formation/South Rumaila Oil Field was presented, in which multiple-point geostatistical methods are used to simulate the lithofacies of a fluvial sand-rich depositional environment. The authors demonstrate the application of these methods





to improve the resolution and realism of the geological model. The results show that the multipoint geostatistical simulation method can reproduce observed depositional patterns and heterogeneity in field data, making Gaussian simulation a valuable tool for reservoir characterization and management in similar depositional environments. The corresponding minimum historical fault model in reservoir modeling has been obtained rapidly. That shows how multi-site statistics reconstruct very complex geographic features (Al-Mudhafar, 2018).

### 3. ORIGINAL OIL IN PLACE (OOIP) CALCULATION AND GEOLOGICAL MODEL CONSTRUCTION

#### 3.1 Original Oil in Place (OOIP) Calculation

Estimating Original Oil in Place (OOIP) The reservoir survey has foundation pillars, which give n geological characteristics. Porosity, saturation, and net-to-gross ratios are important inputs for OOIP calculations. Porosity reflects the bare fraction of the rock mass, while saturation accounts for the pore fraction consumed by hydrocarbons. Net-to-gross ratios, which represent the fraction of reservoir rocks in a given volume, further resolve these estimates. Combining these parameters, OOIP is calculated using the volume equation: OOIP (bbl) = area (acres) × net pay (ft) × porosity × oil saturation × (7758 / formation volume factor) The formation volume factor for oil rates are variable as they evolve from lakes to surface conditions (Najeeb et al., 2020).

$$\text{OOIP} = \frac{7758 A h \phi (1-S_{wc})}{B_{oi}} \quad (30)$$

where:

A is the Area, acres.

H is the Net thickness or height formation, (ft).

$\phi$  is the porosity, fraction.

$S_{wc}$  is the water saturation, fraction.

$B_{oi}$  is the Formation volume faction, (bbl/STB).

To develop the geologic or static model required to characterize and map reservoirs, combine data from multiple sources to create a continuous subsurface model The model relies on well-log data, outcrop analogs, and regional area geological background mainly because it lacks core seismic information. Petrophysical property vertical profiles, such as porosity, resistivity, and gamma-ray intensity, can be obtained from well logs. These logs are utilized to populate the 3D grid cells that make up the model, which captures differences in lithology, porosity, and fluid saturation. Outcrop analogues offer insights into reservoir architecture and heterogeneity by offering real-world geological features that may be extrapolated to subsurface conditions. This allows for more accurate modelling of reservoir architecture and heterogeneity. Incorporating the geological context of a particular location into the model helps to situate it within the larger geological framework. The correctness of the model is contingent on integrating these many data sources, which pave the way for producing a trustworthy representation of reservoir features and spatial distribution (Najeeb et al., 2020). The productivity of the wells was compared before and after stimulation allowing for an accurate estimation of the average productivity of future development wells. We conducted sensitivity analyses on the various well types, patterns,



and spacings using the sector model. We looked into both the practicability and the optimal timing of water injection. Extensive field modelling was used to depict various possibilities for developing the Khasib II field. One piece of advice for the most effective method of expansion is that water flooding will bring the recovery factor down to 35% (**Zhang, 2011**).

## 3.2 Geological Model Construction

### 3.2.1 Lithological and Facies Modeling

The goal of lithological and facies modelling is to depict the spatial distribution of the reservoir's sedimentary facies and various rock types. Lithofacies are given to specific grid cells using well-log data, statistical analysis, and geological concepts. Patterns identified in well logs, such as changes in gamma-ray, resistivity, and neutron porosity, are used to identify and classify diverse lithologies. The model captures the heterogeneity and continuity of lithological units by projecting these patterns laterally and vertically, which is necessary for realistic fluid flow simulations (**Alqassab and Vaughan, 2012**).

### 3.2.2 Property Modeling

Folds, faults, and subsurface structures that affect reservoir dynamics are represented by structural models. In the absence of seismic data, the understanding of architectural complexity is largely based on borehole data and geologic interpretation. Faults can be identified from well logs that show abrupt changes in properties between fault planes important for flow regulation and arrest (**Abdul-Majeed et al., 2020**). Folds are mapped based on well profiles that reflect changes in dip directions at bedding angles. Flow simulations incorporating these structural characteristics are more accurate and provide insight into possible reservoir segmentation (**Najeeb et al., 2020**).

### 3.2.3 Upscaling and Gridding

The definition of a grid spanning the reservoir extent is a necessary step in developing a landscape model. The theoretical and computational efficiency of the model depends on the size of the cells in the grid. Upscaling techniques are used to convert finer geographic information into coarser grid cells of the model. Integrating petrophysical characteristics from small volumes to larger grid cells to maintain overall reservoir characteristics is the focus to increase to bridge the gap between model cell size and well data scale.

## 4 CONCLUSIONS

This comprehensive exploratory study shows the mechanisms by which petrophysical properties influence rock types and geologic properties, with the aim of enhancing reservoir properties. A comprehensive review of previous research and literature has provided many important details. First, exploratory studies emphasize the importance of petrophysical properties such as porosity, rock mass, water saturation, permeability, etc. in classifying rock types. These properties are important indicators of reservoirs no efficiency, hydrocarbon potential, and water behavior. If geologists and engineers understand the relationship between rock material and rock types, they can distinguish between rock types and irregularities in a reservoir.

Second, the reviewed research has shed light on how petrophysical aspects affect the development of geological models. Integrating petrophysical data, rock type classification,



and geology into the modeling process can better represent reservoir bottom structures. This integration ultimately improves reservoir characterization and decision-making for hydrocarbon exploration and production do it through a better understanding of facilitating the diversity of the lakes

Research studies have also shown the importance of improved rock types such as Windland, Lucia Rock Fabric Number, Hydraulic Flow Unit (HFU) etc. These methods improve geological model accuracy and provide knowledge complete with reservoir parameters. By integrating these complex approaches, scholars and practitioners can gain a deeper understanding of the complex relationships between rock properties, rock properties, and reservoir performance.

## NOMENCLATURE

Symbol	Description	Symbol	Description
$V_{cl}$	Clay volume	IGR	Gamma Ray Index
$R_{cl}$	Resistivity of clay	$R_t$	Resistivity of Shaly Sand
$R_{LIM}$	Resistivity of A clean hydrocarbon zone	$V_{cl}$	Volume of clay
SSP	Static and spontaneous log recording at precise intervals (MV)	$R_w$	The Water's resistivity during formation (Ohm-M)
$R_{mf}$	The resistance of the filtrate from mud (ohm-m)	$S_w$	The Water saturation
$n$	The saturation exponent	$\tau$	The tortuosity factor
$\phi_{\tau}$	The porosity	$m$	The cementation factor

## Acknowledgements

The Authors extend appreciation to the Ministry of Oil for its data assistance, as well as to the University of Baghdad. I am thankful for the support received from the Dean's Office of the College of Engineering and the head of the Oil Engineering Department throughout this endeavor.

## Credit Authorship Contribution Statement

Salam Khalid Hasoon: Writing –review & editing, Writing –original draft, Validation, Software. Ghanim M. Farman: Writing –review & editing, Supervision, Methodology, Reviewing & support.

## Declaration of Competing Interest

The authors declare that they have no known competing financial interests or personal relationships that could have appeared to influence the work reported in this paper.

## REFERENCES

Abdallah, W., Ali, F., Valori, A. and Ma, S., 2023. Extracting continuous profiles of archie parameters from downhole measurements. In: *Middle East Oil, Gas and Geosciences Show. OnePetro*. <https://doi.org/10.2118/213947-MS>

Abdul-majeed, Y.N., Ramadhan, A.A. and Mahmood, A.J., 2020. Petrophysical properties and well log interpretations of tertiary reservoir in khabaz oil field/northern Iraq. *Journal of Engineering*, 26(6),



pp.18–34. <http://doi.org/10.31026/j.eng.2020.06.02>.

Abdulkareem, A.N., Hussien, M.Y. and Hasan, H., 2020. Evaluation of petrophysical properties of zubair formation luhais oil field using well logging analysis and archie parameters. *Journal of Engineering*, 26(3), pp.145–159. <http://doi.org/10.31026/j.eng.2020.03.12>.

Abed, A.A. and Hamd-Allah, S.M., 2019. Comparative permeability estimation method and identification of rock types using cluster analysis from well logs and core analysis data in tertiary carbonate reservoir-khabaz oil field. *Journal of Engineering*, 25(12), pp.49–61. <http://doi.org/10.31026/j.eng.2019.12.04>.

Abudeif, A.M., Attia, M.M. and Radwan, A.E., 2016. Petrophysical and petrographic evaluation of sidri member of belayim formation, badri field, Gulf of Suez, Egypt. *Journal of African Earth Sciences*, 115, pp.108–120. <http://doi.org/10.1016/j.jafrearsci.2015.11.028>.

Adeoti, L., Ayolabi, E.A. and James, P.L., 2009. An integrated approach to volume of shale analysis: niger delta example, *Orire Field*.

Adisoemarta, P.S., Anderson, G.A., Frailey, S.M. and Asquith, G.B., 2001. Saturation exponent n in well log interpretation: another look at the permissible range. In: *SPE Permian Basin Oil and Gas Recovery Conference*. SPE. p.SPE-70043. <http://doi.org/10.2118/70043-MS>.

Ahmed, R. and Farman, G.M., 2023a. How to estimate the major petrophysical properties: A review. *Iraqi Journal of Oil and Gas Research (IJGR)*, 3(1), pp.43–58. <http://doi.org/10.55699/ijogr.2023.0301.1037>.

Ahmed, R. and Farman, G.M., 2023b. Evaluating petrophysical properties of Sa'di reservoir in Halfaya oil field, *Iraqi Geol. J.*, pp. 118–126. <https://doi.org/10.46717/igj.56.2D.9ms-2023-10-15>.

Akbar, M.N., 2019. New approaches of porosity-permeability estimations and quality factor q characterization based on sonic velocity, critical porosity, and rock typing. In: *SPE Annual Technical Conference and Exhibition*. OnePetro. <http://doi.org/10.2118/199777-STU>.

Al-Dhafeeri, A.M. and Nasr-El-Din, H.A., 2007. Characteristics of high-permeability zones using core analysis, and production logging data. *Journal of Petroleum Science and Engineering*, 55(1–2), pp.18–36. <http://doi.org/10.1016/j.petrol.2006.04.019>.

Al-Hilali, M.M., Zein Al-Abideen, M.J., Adegbola, F., Li, W. and Avedisian, A.M., 2015. A petrophysical technique to estimate archie saturation exponent (n); case studies in carbonate and shaly-sand reservoirs–iraqi oil fields. In: *SPE Annual Caspian Technical Conference*. SPE. p.SPE-177331. <http://doi.org/10.2118/177331-MS>.

Al-Mudhafar, W.J., 2018. Multiple–point geostatistical lithofacies simulation of fluvial sand–rich depositional environment: A case study from Zubair formation/South Rumaila oil field. *SPE Reservoir Evaluation & Engineering*, 21(01), pp.39–53. <http://doi.org/10.2118/187949-PA>.

Al-Ofi, S., Ma, S., Kesserwan, H. and Jin, G., 2022. A new approach to estimate archie parameters m and n independently from dielectric measurements. In: *SPWLA Annual Logging Symposium*. SPWLA. p.D031S004R002. <http://doi.org/10.30632/SPWLA-2022-0002>.

Alameedy, U., Farman, G.M. and Al-Tamemi, H., 2023. Mineral inversion approach to improve Ahdeb oil field's mineral classification. *The Iraqi Geological Journal*, pp.102–113. <http://doi.org/10.46717/igj.56.2B.8ms-2023-8-17>.

Ali, H.Y., Farman, G.M. and Hafiz, M.H., 2021. Study of petrophysical properties of the yamama



formation in Siba oilfield. *Iraqi Geological Journal*, 54(2), pp.39–47. <http://doi.org/10.46717/IGJ.54.2C.4MS-2021-09-23>.

Almazroui, M., Saeed, S., Saeed, F., Islam, M.N. and Ismail, M., 2020. Projections of precipitation and temperature over the South Asian countries in cmip6. *Earth Systems and Environment*, 4, pp.297–320. <http://doi.org/10.1007/s41748-020-00157-7>.

Alqassab, H. and Vaughan, L., 2012. Impact of facies modeling on reservoir performance forecasting: a comparison between discrete modeling and mixed lithology approaches. In: *SPE Kuwait International Petroleum Conference and Exhibition*. SPE. p.SPE-163293. <http://doi.org/10.2118/163293-MS>.

Al Jawad, M.S. and Tariq, B.Z., 2019. Estimation of cutoff values by using regression lines method in Mishrif reservoir/Missan oil fields. *Journal of Engineering*, 25(2), pp.82–95. <http://doi.org/10.31026/j.eng.2019.02.06>.

Al Kattan, W., Jawad, S.N.A.L. and Jomaah, H.A., 2018. Cluster analysis approach to identify rock type in tertiary reservoir of Khabaz oil field case study. *Iraqi Journal of Chemical and Petroleum Engineering*, 19(2), pp.9–13.

Aquino-López, A., Mousatov, A., Markov, M. and Kazatchenko, E., 2015. Modeling and inversion of elastic wave velocities and electrical conductivity in clastic formations with structural and dispersed shales. *Journal of Applied Geophysics*, 116, pp.28–42. <http://doi.org/10.1016/j.jappgeo.2015.02.013>.

Archie, G.E., 1950. Introduction to petrophysics of reservoir rocks, *AAPG bulletin*, <http://doi.org/10.1306/3D933F62-16B1-11D7-8645000102C1865D>.

Bassiouni, Z., 1994. Theory, measurement, and interpretation of well logs. doherty memorial fund of aime. *Society of petroleum engineers*.

Bateman, R.M., 2020. Formation evaluation with pre-digital well logs. *Elsevier*.

Bhatti, A.A., Ismail, A., Raza, A., Gholami, R., Rezaee, R., Nagarajan, R. and Saffou, E., 2020. Permeability prediction using hydraulic flow units and electrofacies analysis. *Energy Geoscience*, 1(1–2), pp.81–91. <http://doi.org/10.1016/j.engeos.2020.04.003>.

Bose, S., Myers, M.T., Chen, P. and Thakur, G., 2019. Application of an integrated petrophysical modeling to improve log based reservoir characterization and oil in-place estimate of a fresh water Shaly sand reservoir. In: *SPWLA Annual Logging Symposium*. SPWLA. p.D053S018R003. [http://doi.org/10.30632/T60ALS-2019\\_DDDDD](http://doi.org/10.30632/T60ALS-2019_DDDDD).

Burke, J.A., Campbell, R.L. and Schmidt, A.W., 1969. The litho-porosity cross plot a method of determining rock characteristics for computation of log data. In *SPE Illinois Basin Regional Meeting*. <http://doi.org/10.2118/2771-MS>.

Burke, J.A., Campbell, R.L. and Schmidt, A.W., 1969. The litho-porosity cross plot a method of determining rock characteristics for computation of log data. In: *SPE Illinois Basin Regional Meeting*. OnePetro. <http://doi.org/10.2118/2771-MS>.

Burns, A.H.C.R.E.P.S., 2013. Gas shale characterization - results of the mineralogical, lithological and geochemical analysis of cuttings samples from radioactive silurian shales of a palaeozoic basin, SW Algeria. *Paper presented at the North Africa Technical Conference and Exhibition, Cairo, Egypt*. <http://doi.org/10.2118/164695-MS>.

Cannon, S., 2015. *Petrophysics: A practical guide*. John Wiley & Sons.





- Chen, H., Sarili, M., Wang, C., Naito, K., Morikami, Y., Shabibi, H., Frese, D. and Pfeiffer, T., 2020. Calibrated formation water resistivity sensor. In: *SPWLA Annual Logging Symposium*. SPWLA. p.D083S008R003. <http://doi.org/10.30632/SPWLA-5021>.
- Cornish, R., 2007. Statistics: Cluster analysis. *Mathematics Learning Support Centre*, 3, pp.1–5.
- Díaz, G., Mendez, F., Alarcon, N., Paris, M., Lopez, A. and Gade, S., 2016, June. Comparative study of pulsed-neutron derived openhole and casedhole lithology, mineralogy and total organic carbon in unconventional reservoir. In *SPWLA Annual Logging Symposium* (pp. SPWLA-2016). SPWLA.
- Doveton, J.H., 1994. Geologic log analysis using computer methods. *Canadian Society of Petroleum Geologists*. <http://doi.org/10.1306/CA2580>.
- Ferguson, G.J., Willis, J.J., McIntosh Jr, D.S., Zwennes, J.W., Pasley, J. and Goettel, G.M., 2018. Influence of shale distribution types on the effective porosity of sandstone reservoirs. *Gulf Coast Association of Geological Societies Transactions*, 67.
- Hamada, G.M., 1996. An integrated approach to determine shale volume and hydrocarbon potential in shaly sand. In *SCA International Symposium*.
- Hosseini, E., Gholami, R. and Hajivand, F., 2019. Geostatistical modeling and spatial distribution analysis of porosity and permeability in the Shurijeh-b reservoir of Khangiran gas field in Iran. *Journal of Petroleum Exploration and Production Technology*, 9(2), pp.1051–1073.
- Hossin, A., 1965. Feature article calculation of useful porosity in shaly sandstones. In: *SPWLA Annual Logging Symposium*. SPWLA. p.SPWLA-1965.
- Hussein, R.A.M. and Ahmed, M.E.B., 2012. Petrophysical evaluation of shaly sand reservoirs in Palouge-fal oilfield, melut basin, south east of Sudan. *Journal of science and technology*, 13(2).
- Kamel, M.H. and Mohamed, M.M., 2006. Effective porosity determination in clean/shaly formations from acoustic logs with applications. *Journal of Petroleum Science and Engineering*, 51(3–4), pp.267–274. <http://doi.org/10.1016/j.petrol.2006.01.007>.
- Kennedy, D., 2016. Conducting connected porosity: a concept for unifying resistivity-porosity models. *Paper presented at the SPWLA 57th Annual Logging Symposium, Reykjavik, Iceland*.
- Kennedy, D. and Garcia, F., 2019. Tutorial: introduction to resistivity principles for formation evaluation: A tutorial primer. *Petrophysics*, 60(02), pp.208–227. <http://doi.org/10.30632/PJV60N2-2019t2>.
- Ko Ko Kyi, 2019. Petrophysical cutoff a touchy subject. *Presentation course published*.
- Kolodzie Jr, S., 1980. Analysis of pore throat size and use of the waxman-smits equation to determine oip in spindle field, colorado. In: *SPE Annual Technical Conference and Exhibition? SPE*. p.SPE-9382. <http://doi.org/10.2118/9382-MS>.
- Lorentzen, R.J., Naevdal, G., Valles, B., Berg, A.M. and Grimstad, A.-A., 2005. Analysis of the ensemble kalman filter for estimation of permeability and porosity in reservoir models. In: *SPE Annual Technical Conference and Exhibition? SPE*. p.SPE-96375. <http://doi.org/10.2118/96375-MS>.
- Lucia, F.J., Kerans, C. and Jennings Jr, J.W., 2003. Carbonate reservoir characterization. *Journal of Petroleum Technology*, 55(06), pp.70–72. <http://doi.org/10.2118/82071-JPT>.
- Mabrouk, W.M., Soliman, K.S. and Anas, S.S., 2013. New method to calculate the formation water resistivity (Rw). *Journal of Petroleum Science and Engineering*, 104, pp.49–52.



<http://doi.org/10.1016/j.petrol.2013.03.010>.

Mahdi, Z.A. and Farman, G.M., 2023a. A review on models for evaluating rock petrophysical properties. *Iraqi Journal of Chemical and Petroleum Engineering*, 24(1), pp.125–136. <http://doi.org/10.31699/IJCPE.2023.1.14>.

Mahdi, Z.A. and Farman, G.M., 2023b. Estimation of petrophysical properties for Zubair reservoir in Abu-Amood Oil field. *Iraqi Geological Journal*, 56(1), pp.32–39. <http://doi.org/10.46717/igj.56.1B.3ms-2023-2-11>.

Mahdi, Z.A. and Farman, G.M., 2023c. 3D Geological Model for Zubair reservoir in Abu-Amood oil field. *Iraqi Geological Journal*, 56(1b), pp. 40-50. <http://doi.org/10.46717/igj.56.1B.4ms-2023-2-12>.

Maignant, G. and Staccini, P., 2018. Statistical, Mapping and Digital Approaches in Healthcare. *Elsevier*.

Mamaseni, W.J., Naqshabandi, S.F. and Al-Jaboury, F.K., 2018. Petrophysical properties of the early cretaceous formations in the Shaikhan oilfield/northern Iraq. *Earth Sciences Research Journal*, 22(1), pp.45–52.

Mazzullo, S.J., Rieke, H.H. and Chilingarian, G. V, 1996. Carbonate reservoir characterization: A geologic-engineering analysis, part II. *Elsevier*.

Mihai, D. and Mocanu, M., 2015. Statistical considerations on the k-means algorithm. *Annals of the University of Craiova-Mathematics and Computer Science Series*, 42(2), pp.365–373.

Mohamad, A.M. and Hamada, G.M., 2017. Determination techniques of archie's parameters: a, m and n in heterogeneous reservoirs. *Journal of Geophysics and Engineering*, 14(6), pp.1358–1367.

Najeeb, M., Kadhim, F.S. and Saed, G.N., 2020. Using different methods to predict oil in place in Mishrif Formation/Amara oil field. *Iraqi Journal Chemical Petroleum Engineering*, 21(1), pp.33–38. <http://doi.org/10.31699/IJCPE.2020.1.5>.

Najlaa Fathi Hasan, 2021., Evaluation of reservoir characterization with 3D modeling in Mishrif formation - Amara oil field, *M.Sc. thesis, Petroleum Engineering, University of Baghdad*.

Ngo, V.T., Lu, V.D., Nguyen, M.H., Hoang, T.M., Nguyen, H.M. and Le, V.M., 2015. A comparison of permeability prediction methods using core analysis data. In: *SPE Reservoir Characterisation and Simulation Conference and Exhibition? SPE*. p.D011S001R003. <http://doi.org/10.2118/175650-MS>.

Nielsen, A.A., 2009. Geostatistics and analysis of spatial data. *Informatics and Mathematical Modelling, Technical University of Denmark, DTU*, pp.7–12.

Osterloh, W.T., Mims, D.S. and Meddaugh, W.S., 2013. Probabilistic forecasting and model validation for the first-eocene large-scale pilot Steamflood, Partitioned Zone, Saudi Arabia and Kuwait. *SPE Reservoir Evaluation & Engineering*, 16(01), pp.97–116. <http://doi.org/10.2118/150580-PA>.

Paul, F. and Gaffney, W., 2003. The application of cutoffs in integrated reservoir studies. *Society of Petroleum Engineers*, 84387, pp.1–16. <http://doi.org/10.2118/95428-PA>.

Pickett, G.R., 1966. A review of current techniques for determination of water saturation from logs'. *Journal of Petroleum Technology*. <http://doi.org/10.2118/1446-PA>.

Pittman, E.D., 1992. Relationship of porosity and permeability to various parameters derived from mercury injection-capillary pressure curves for sandstone. *AAPG bulletin*, 76(2), pp.191–198. <http://doi.org/10.1306/BDF87A4-1718-11D7-8645000102C1865D>.



- Pius, T.O. and Olamigoke, O., 2020. Investigating the correlation between water saturation obtained from cased-hole saturation tool measurements and produced water cut in strong water drive reservoirs. In: *SPE Nigeria Annual International Conference and Exhibition. OnePetro*. <http://doi.org/10.2118/203620-MS>.
- Policky, B.R. and Iverson, W.P., 1988. Water resistivity from spontaneous potential logs in the minnelusa formation, powder river basin, wyoming. In: *SPE Rocky Mountain Petroleum Technology Conference/Low-Permeability Reservoirs Symposium. SPE*. p.SPE-17516. <http://doi.org/10.2118/17516-MS>.
- Porras, J.C., Barbato, R. and Salazar, D., 2001. Upscaling from core data to production: Closing the cycle. A Case Study in the Santa Barbara and Piritall Fields, Eastern Venezuela Basin. In: *International Symposium of the SCA. Murrayfield, Edinburgh*. pp.17–19.
- Qiu, M. and Yi, J., 2023. Reservoir rock typing: integration of geological attributes and petrophysical properties: Case Study from Yamama Reservoir. In: *SPE Gas & Oil Technology Showcase and Conference. SPE*. p.D021S024R002. <http://doi.org/10.2118/214247-MS>.
- Rezaee, M.R., Kadkhodaie-Ilkhchi, A. and Alizadeh, P.M., 2008. Intelligent approaches for the synthesis of petrophysical logs. *Journal of Geophysics and Engineering*, 5(1), pp.12–26. <http://doi.org/10.1088/1742-2132/5/1/002>.
- Riazi, Z., 2018. Application of integrated rock typing and flow units identification methods for an iranian carbonate reservoir. *Journal of Petroleum Science and Engineering*, 160, pp.483–497. <http://doi.org/10.1016/j.petrol.2017.10.025>.
- Salem, H.S. and Chilingarian, G. V, 1999. The cementation factor of archie's equation for shaly sandstone reservoirs. *Journal of Petroleum Science and Engineering*, 23(2), pp.83–93. [http://doi.org/10.1016/S0920-4105\(99\)00009-1](http://doi.org/10.1016/S0920-4105(99)00009-1).
- Salman, O., Al-Fatlawi, O. and Al-Jawad, S., 2023. Reservoir characterization and rock typing of carbonate reservoir in the southeast of Iraq. *Iraqi Geological Journal*, 56(1), pp.221–237. <http://doi.org/10.46717/igi.56.1A.17ms-2023-1-29>.
- Schön, 2015. Physical properties of rocks: Fundamentals and principles of Petrophysics. Second Edition. *Elsevier*.
- Shahi, M., Salehi, M.M. and Kamari, M., 2018. New correlation for estimation of cementation factor in asdari carbonate rock reservoirs. *Egyptian Journal of Petroleum*, 27(4), pp.663–669. <http://doi.org/10.1016/j.ejpe.2017.10.002>.
- Shedid, S.A. and Saad, M.A., 2017. Comparison and sensitivity analysis of water saturation models in shaly sandstone reservoirs using well logging data. *Journal of Petroleum Science and Engineering*, 156, pp.536–545. <http://doi.org/10.1016/j.petrol.2017.06.005>.
- Simandoux, P., 1963. Dielectric measurements on porous media, application to the measurements of water saturation: study of behavior of argillaceous formations. *Revue de L'institut Francais du Petrole*, 18(Supplementary Issue), pp.193–215.
- Singh, K.H. and Joshi, R.M., 2020. Petro-physics and rock physics of carbonate reservoirs. *Springer*.
- Skalinski, M. and Kenter, J.A.M., 2015. Carbonate petrophysical rock typing: integrating geological attributes and petrophysical properties while linking with dynamic behaviour. *Geological Society, London, Special Publications*, 406(1), pp.229–259. <http://doi.org/10.1144/SP406.6>.



- Su, K., Barlet, P., Borgomano, J.V.M., Castets, M., Caillet, C., Okullo, R., Azevedo, C., Ferreira, F., Beele, M. and Coelho, D., 2022. Short and long-term fracture permeability tests under stress on pre-salt low permeability carbonates after acid treatment or with proppants. *In: Abu Dhabi International Petroleum Exhibition and Conference. SPE.* p.D032S170R007. <http://doi.org/10.2118/211404-MS>.
- Svirsky, D., Ryazanov, A., Pankov, M., Corbett, P.W.M. and Posysoev, A., 2004. Hydraulic flow units resolve reservoir description challenges in a siberian oil field. *In: SPE Asia Pacific conference on integrated modelling for asset management. SPE.* p.SPE-87056. <http://doi.org/10.2118/87056-MS>.
- Taslimi, M., Kazemzadeh, E. and Kamali, M.R., 2008. Determining rock mass permeability in a carbonate reservoir, southern iran using hydraulic flow units and intelligent systems. *In Tehran, Iran, Wseas International Conference On Geology And Seismology (Ges' 08), Cambridge, UK.* <http://doi.org/10.1111/j.1747-5457.2009.00435.x>.
- Wang, Y., Cao, Y., Song, G., Song, L., Yang, T. and Zhang, S., 2014. Analysis of petrophysical cutoffs of reservoir intervals with production capacity and with accumulation capacity in clastic reservoirs. *Petroleum Science*, 11, pp.211–219.
- Winsauer, W.O., Shearin Jr, H.M., Masson, P.H. y and Williams, M., 1952. Resistivity of brine-saturated sands in relation to pore geometry. *AAPG Bulletin*, 36(2), pp.253–277. <http://doi.org/10.1306/3D9343F4-16B1-11D7-8645000102C1865D>.
- Yaming Zou; Wenling Liu; Hui Zhou; Shoujun Guan; Hanming Chen, 2013. A new implementation procedure of sequential gaussian simulation in stochastic seismic inversion. *Paper presented at the 2013 SEG Annual Meeting, Houston, Texas.* <http://doi.org/10.1190/segam2013-0490.1>.
- Yarmohammadi, S., Kadkhodaie, A. and Shirzadi, A., 2013. Determination of hydraulic flow units in sandstone reservoirs by integration of petrophysical data, well logs and seismic inversion results. *In: the Second Conference on Hydrocarbon Reservoirs and Related Industries, Tehran, Iran.*
- Zhang, Y., 2011. Introduction to geostatistics-course notes. *Laramie: University of Wyoming, Department of Geology and Geophysics.*

## دمج الخصائص البتروفيزيائية، وتشكيل الصخور، والنمذجة الجيولوجية لتعزيز توصيف المكان: مراجعة شاملة

سلام خالد حسون\*، غانم مديح فرمان

قسم هندسة النفط، كلية الهندسة، جامعة بغداد، بغداد، العراق

### الخلاصة

توصيف المكان هو عنصر مهم في استكشاف وإنتاج المواد الهيدروكربونية، الأمر الذي يتطلب دمج التخصصات المختلفة لنمذجة دقيقة تحت السطح. تتعمق هذه الورقة البحثية الشاملة في التفاعل المعقد بين المواد الصخرية وتقنيات تكوين الصخور وتقنيات النمذجة الجيولوجية لتحسين جودة المكن. وتلعب الورقة دوراً مهماً تهيمن عليه العوامل البتروفيزيائية مثل المسامية وحجم الصخر الزيتي ومحتوى الماء والنفاذية - وهي عوامل مهمة. مؤشرات خصائص الخزان، وسلوك السوائل، وإمكانات الهيدروكربون. يدرس البحث تقنيات فهرسة الصخور المختلفة، مع التركيز على تقنيات تجميع الصخور وخرائط التنظيم الذاتي (SOMS) لتحديد الوجوه الصخرية المحددة والشاذة علاوة على ذلك، يستكشف البحث اعتماد أساليب متقدمة لتسجيل الصخور، بما في ذلك وحدات التدفق الهيدروليكي (HFU) مما يوفر فهماً دقيقاً لعدم تجانس الخزان والمساهمة في التنبؤ بديناميكيات التدفق. يتضمن القسم النهائي النماذج الجيولوجية الهيكلية والبيانات البتروفيزيائية وتصنيف أنواع الصخور المجمعة والبيانات المكانية لتمثيل هيكل قاع الخزان بشكل أفضل، ويوفر مورداً قيماً للباحثين والجيولوجيين والمهندسين الذين يسعون إلى توصيف الخزانات واتخاذ القرارات المثلى بشأن استكشاف وإنتاج الهيدروكربون، وهو عنصر مهم في استكشاف وإنتاج الهيدروكربون، الأمر الذي يتطلب دمج التخصصات المختلفة لنمذجة دقيقة تحت السطح.

**الكلمات المفتاحية:** الخصائص البتروفيزيائية، خصائص الصخور، التكتلات، نماذج التربة، وخصائص المكان.